

Role of muscle damage on loading at the level adjacent to a lumbar spine fusion: a biomechanical analysis

Masoud Malakoutian¹ · John Street² · Hans-Joachim Wilke³ · Ian Stavness⁴ · Marcel Dvorak² · Sidney Fels⁵ · Thomas Oxland^{1,2}

Received: 2 September 2015 / Revised: 8 April 2016 / Accepted: 29 June 2016 / Published online: 27 July 2016
© Springer-Verlag Berlin Heidelberg 2016

Abstract

Purpose It is well established that posterior spinal surgery results in damage to the paraspinal musculature. The effects of such iatrogenic changes on spinal loading have not been previously investigated, particularly at levels adjacent to a spinal fusion. Therefore, the objective of this study was to investigate the effect of simulated muscle damage on post-operative spinal loading at the adjacent levels to a spinal fusion during upright postures using a mathematical model.

Methods A musculoskeletal model of the spine using ArtiSynth with 210 muscle fascicles was used to predict spinal loading in an upright posture. The loading at L1–L2 and L5–S1 were estimated before and after simulated paraspinal muscle damage (i.e., removal of muscle attachments at L2–L5) along the lumbar spine, both with a spinal fusion at L2–L5 and without a spinal fusion.

Results The axial compressive forces at the adjacent levels increased after simulated muscle damage, with the largest

changes being at the rostral level (78 % increase in presence of spinal fusion; 73 % increase without spinal fusion) compared to the caudal level (41 % in presence of fusion and 32 % without fusion). Shear forces increased in a similar manner at both the rostral and caudal levels. These changes in loading were due to a redistribution of muscle activity from the local lumbar to the global spinal musculature.

Conclusions The results suggest that the paraspinal muscles of the lumbar spine play an important role in adjacent segment loading of a spinal fusion, independent of the presence of rigid spinal instrumentation.

Keywords Muscle damage · Adjacent segment degeneration · Lumbar spine · Biomechanics · Musculoskeletal model · ArtiSynth

Introduction

The degeneration of the segment adjacent to a lumbar spine fusion is commonly seen following fusion surgery [1]. Prevention of adjacent segment degeneration (ASD) requires an understanding of its etiology. While some believe this phenomenon is simply an expression of the natural history of multi-segmental spinal column degeneration [2–4], many believe ASD represents an accelerated degenerative process that can be explained through biomechanical modeling [1, 5–7].

Animal studies have shown that increased loading across the intervertebral disc accelerates disc degeneration [8–12]. Therefore, any factor that changes normal loading at the adjacent levels may have an influence on the development of ASD. One factor that may cause that change is paraspinal muscle dysfunction.

✉ Thomas Oxland
toxland@exchange.ubc.ca

¹ Department of Mechanical Engineering, University of British Columbia, Vancouver, BC, Canada

² Department of Orthopaedics, University of British Columbia, ICORD, Blusson Spinal Cord Centre, 5th Floor, 818 West 10th Avenue, Vancouver, BC V5Z 1M9, Canada

³ Institute of Orthopaedic Research and Biomechanics, Center of Musculoskeletal Research, University of Ulm, Ulm, Germany

⁴ Department of Computer Science, University of Saskatchewan, Saskatoon, SK, Canada

⁵ Department of Electrical and Computer Engineering, University of British Columbia, Vancouver, BC, Canada

Paraspinal muscles are vital for the effective functioning of the spine, yet we know surprisingly little about their behavior in the setting of preoperative deconditioning or in post-operative muscle behavior. It is likely that many patients prior to spine surgery have dysfunctional paraspinal musculature, and that this is exacerbated due to iatrogenic changes following surgery. For example, we know that paraspinal muscle function is abnormal in a range of prevalent clinical conditions including acute and chronic low back pain [13–16], spinal stenosis [17, 18], and degenerative spondylolisthesis [19]. In addition, it is well established that spine surgery can damage posterior musculature through resection of the paraspinal muscles from the posterior elements or simple retraction of paraspinal muscles to the side which is done to provide surgical exposure [14, 20–22]. Spinal muscle damage after posterior fusion surgeries has been manifested in forms of loss of cross-sectional area (CSA) [23], atrophy [24, 25], altered muscle activations [26, 27], and reduced muscle strength [20, 24, 28, 29]. The effect of paraspinal muscle damage on spinal forces and moments has not been studied previously, particularly with respect to the adjacent segment changes.

Many *in vitro* biomechanical studies have been conducted to address possible abnormal biomechanical changes at the adjacent levels to a spinal fusion. Most of these studies make assumptions about the post-operative spine that are not necessarily valid. For example, the popular Hybrid method assumes that the patient's post-operative spinal motion is the same as it was pre-operatively [30]. A recent review of *in vivo* kinematic studies shows that this assumption appears to be false as the majority of subjects in carefully done clinical studies demonstrated lower overall lumbar spine range of motion than pre-operatively [31, 32]. Further, biomechanical studies conducted in the laboratory use either a stiffness (displacement-controlled) or a flexibility (load-controlled) loading protocol to address adjacent segment changes. Both protocols yield obvious results as noted recently in another review paper [33], wherein excessive loading at adjacent levels is predicted by stiffness approaches [34–36] and no changes are predicted by flexibility approaches [37–41]. Therefore, we are in need of alternative approaches to assess the biomechanical changes at adjacent levels to spinal instrumentation in the lumbar spine.

Musculoskeletal dynamic models have been described as effective tools to provide insight into the functioning of the entire spine [42–48]. From our perspective, they provide an ideal tool with which to assess post-operative muscle dysfunction on the levels adjacent to a spinal fusion. Bresnahan et al. [48] used the musculoskeletal model developed by de Zee et al. [45] to investigate the effect of the reduction of muscle cross-sectional areas on muscle recruitment strategy and observed a substantial

change in estimated muscle activation pattern. However, they did not report on spinal loading. Also the model that they used for their analysis did not include intervertebral disc stiffness, ligaments, and muscle force–length curves. The purpose of our study was to investigate the effect of muscle damage on post-operative spinal loading at the adjacent levels to a spinal fusion during upright postures by using a recently developed physiological musculoskeletal model of the lumbar spine [49].

Materials and methods

Musculoskeletal model

The musculoskeletal model of the lumbar spine used ArtiSynth (www.artisynth.org), an open source biomechanical modeling toolkit. This computer software was developed at the University of British Columbia and can combine multi-body dynamics and finite element methods in a fast and convenient fashion [50–52].

A brief description of the current model follows [49]. The bone and muscle geometries were taken from a recent study by Christophy et al. [46], in which muscle parameters are incorporated for a full Hill-type musculotendon model including the tendon ratios and the pennation angles [53]. The five lumbar vertebrae were modeled as rigid bodies that could move, the thoracic vertebrae and ribcage were modeled as a single rigid body fixed to the L1 vertebra, and the sacrum and pelvis were fixed to the ground. The mechanical behavior of the lumbar functional spinal units (i.e., a pair of adjacent vertebrae, connecting ligaments, facet joints, and intervertebral disc) was modeled as a 6×6 stiffness matrix [54], with only diagonal terms modeled due to lack of experimental data in the literature. The rotational stiffness terms were taken from the study by Heuer et al. [55], while the translational terms were adopted from Gardner - Morse and Stokes's study [56]. Muscle groups that could influence the loading at the lumbar spine were modeled and these included the erector spinae (eight fascicles for iliocostalis lumborum pars lumborum, 16 fascicles for iliocostalis lumborum pars thoracis, 10 fascicles for longissimus thoracis pars lumborum, and 42 fascicles for longissimus thoracis pars thoracis), multifidus (50 fascicles), psoas major (22 fascicles), quadratus lumborum (36 fascicles), internal oblique (12 fascicles), external oblique (12 fascicles), and rectus abdominis (two fascicles), which totalled 210 muscle fascicles. Hill-type muscle models were used and the muscle force–length and force–velocity curves were taken from the study by Millard et al. [57] and tendons were assumed to be rigid. We modeled the rectus sheath as a rigid body connected to the sacrum through a hinge joint and we

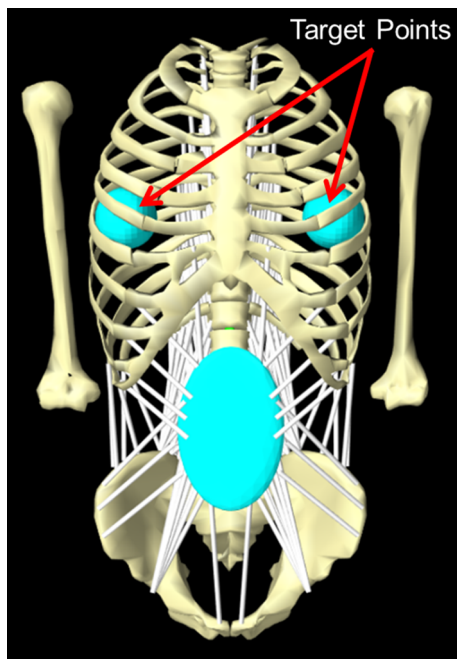


Fig. 1 Symmetric target points in the rib cage specified for tracking the motion of the thorax

modeled the mechanical effect of the intraabdominal pressure as an upward force fixed to the thorax (i.e., moving with it). The force was considered to be 60 N for normal standing [58].

Forward dynamics-assisted data tracking was implemented in a way that a set of weighted cost functions were combined as a total cost function and minimized per each time step through quadratic programming. The cost function ensured that the model-generated velocity was closest to the desired velocity for tracking a target trajectory and that muscle redundancy was addressed while limiting overall muscle activation and ensuring smoother muscle activation over time [59].

In ArtiSynth, forward dynamics-assisted data tracking is coded in a way so that the trajectories of multiple points can be tracked. We specified two target points in our model, whose locations were symmetric with respect to the sagittal plane and both belonged to the ribcage (Fig. 1).

The detailed validation of the model is described elsewhere [49]. The model was able to predict axial forces at L4–L5 that had the same ratio between them as had the three measured intradiscal pressures in the study by Wilke et al. [60] (see Table 5 in [49]).

Study design

To study the effect of spinal muscle damage on spinal loading, we designed two model scenarios. The first scenario (No Fusion) consisted of two models: one

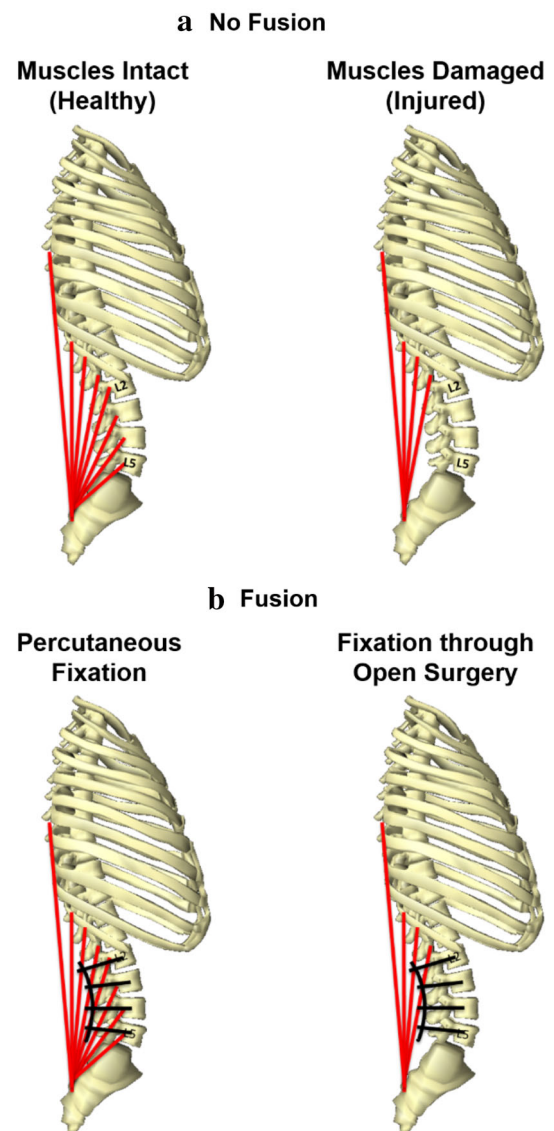


Fig. 2 **a** No fusion scenario of the study design: comparing the spinal loads between a healthy subject and a patient with dysfunctional lumbar musculature (muscles are conceptually drawn in this figure, but in the model the complicated architecture of the muscles is implemented). **b** Fusion scenario of the study design: comparing the spinal loads between a patient receiving percutaneous pedicle screw fixation and a patient undergoing open fusion surgery (muscles are conceptually drawn in this figure, but in the model the complicated architecture of the muscles is implemented)

representing the spine of a healthy subject with intact muscles, while the other characterizing the spine of that subject after a sham surgery, in which the muscles were detached from L2 to L5 (Fig. 2a). Both models were asked to stay upright by prescribing the same target positions. The resulting forces at the intervertebral joints of the models were contrasted. The second scenario (Fusion) was similar to the first, except both models included a simulated spinal fusion: one represented the spine of a patient

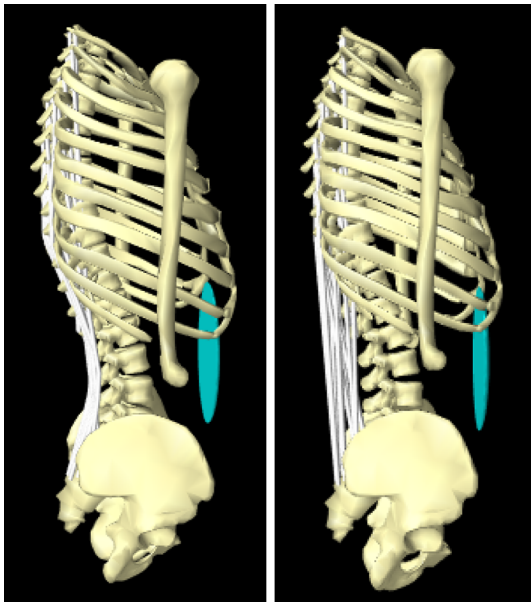


Fig. 3 Simulation of iatrogenic muscle damage to the longissimus thoracis pars thoracis. For fascicles with multiple attachment points, the points that were located at injury levels were removed and the remaining points were reconnected together to again form that fascicle

receiving minimally invasive fusion surgery with percutaneous pedicle screw fixation where posterior muscles are kept intact, and the other typified a patient undergoing open fusion surgery where muscles were detached from the instrumented vertebrae (Fig. 2b).

Note that in order to simulate muscle damage, we treated muscle fascicles of our model in two ways. If a fascicle had only two attachment points and at least one of them was on the injured levels, that fascicle was removed from the model. But if a fascicle had multiple attachment points, only the points that were located at the injury levels were removed and the remaining points were connected together again to form that fascicle (Fig. 3).

Also note that instead of modeling flexible screws and rods, we assumed that the fusion was complete and therefore we treated the instrumented vertebrae (here L2–L5) as one rigid body by fixing them together.

To compare the muscle geometries between the healthy and injured models, we calculated muscle PCSA at each spinal level by summing up the PCSA of all fascicles that passed that level. Each vertebral level was defined by a transverse plane passing through the midpoint of the line connecting the centroids of the two vertebrae adjacent to that plane (Fig. 4). Any fascicle that crossed the plane was included. Therefore, the method was effective for levels L1–L2, L2–L3, and L3–L4, but not for L4–L5 or L5–S1. For these two lowest levels the transverse plane

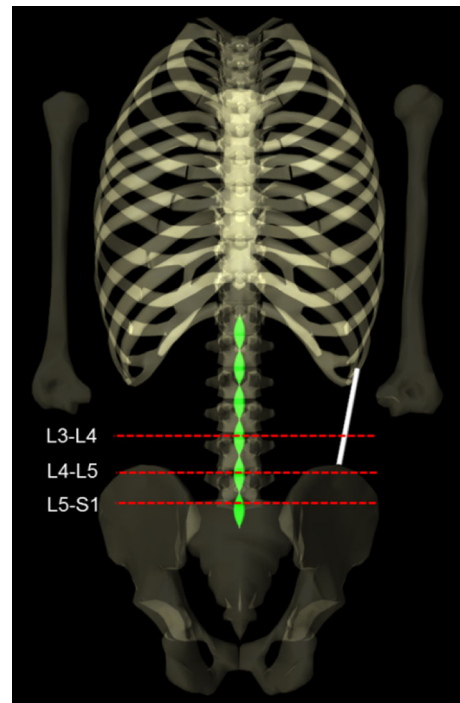


Fig. 4 Definition of each spinal level for calculation of muscle physiological cross sectional areas (PCSA). Each vertebral level was defined by a transverse plane passing through the midpoint of the line connecting the centroids of the two vertebrae adjacent to that plane. The method was effective for levels L1–L2, L2–L3, and L3–L4, but not for L4–L5 and L5–S1. For those two lowest levels the transverse plane cuts through the pelvis, therefore the fascicles with origins on the superior aspect of the pelvis were not considered

cuts through the pelvis; therefore, the fascicles with origins on the superior aspect of the pelvis were not included (Fig. 4).

Results

For the No Fusion scenario, the axial and shear forces at the adjacent vertebral levels (i.e., L1–L2 and L5–S1) increased with muscle damage (Fig. 5a). The increase in the axial force was larger at the rostral level L1–L2 (73 % increase; 483 N) than at the caudal level L5–S1 (32 % increase, 307 N), while the percentage increase in the shear force was similar at both levels (rostral 74 % increase; caudal 85 % increase). The magnitude of flexion–extension moments applied on adjacent levels, however, were small.

The same trend was observed for the Fusion scenario where both the axial and shear forces increased at the adjacent levels with muscle damage with the larger increase in the axial force being at the rostral adjacent level (78 % increase; 610 N) than at the caudal one (41 % increase; 438 N). As in the No Fusion scenario, the shear

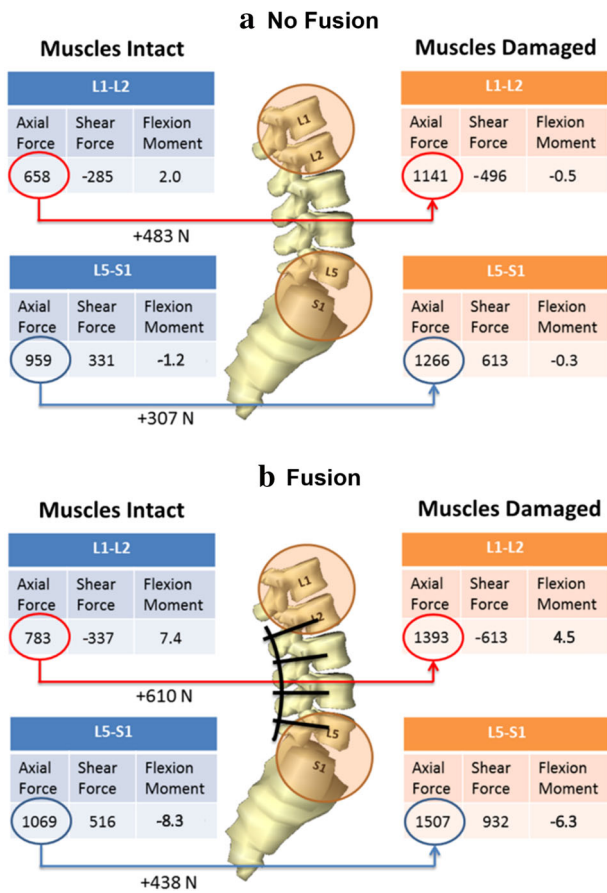


Fig. 5 **a** Predicted spinal loads at the adjacent levels for No Fusion scenario. Forces are in N, moments are in Nm, and positive values for shear forces point to the anterior direction. **b** Predicted spinal loads at the adjacent levels for Fusion scenario. Forces are in N, moments are in Nm, and positive values for shear forces point to the anterior direction

force percentage increases were similar at both levels (rostral 82 % increase; caudal 81 % increase) (Fig. 5b).

We did further analysis to determine the reason for a larger increase in the axial force at the rostral adjacent level in comparison to the caudal one. Since the trends of the results were similar in both scenarios, we only explored the No Fusion scenario in more detail. The loads at each intervertebral level were compared with and without muscle damage (Fig. 6), as were the PCSA and individual muscle group forces crossing the L1–L2 (Fig. 7a) and L3–L4 (Fig. 7b) levels, respectively.

When comparing the PCSAs of the muscle groups between the healthy and muscle damage models, we observed that while at L1–L2, the muscle damage only reduced the PCSAs of QL and LTpT [i.e., area change: QL 163 mm² (39 %), LTpT 369 mm² (17 %)], at L3–L4 it led to substantial reduction of PCSA of MF, ILpL, and LTpL in addition to QL and LTpT [i.e., area change: MF 750 mm² (80 %), ILpL 665 mm² (76 %), LTpL 381 mm² (71 %), QL 358 mm² (58 %), and LTpT 411 mm² (20 %)].

These differences in PCSA reductions led to altered muscle force distributions (Fig. 7a, b). Considering the muscle groups as three major groups: IO and EO as abdominal muscles; LTpT and ILpT as global muscles (which span the entire lumbar spine and are inserted on thoracic region); and finally MF, LTpL, and ILpL as local muscles (which are attached to different levels of the lumbar spine), our results showed that after injury the sum of forces in IO and EO increased by 341 N (189 %) at both L1–L2 and L3–L4 levels. Similarly the sum of forces in LTpT and ILpT (global muscles) increased at both levels [145 N (68 %) for L1–L2 and 148 N (71 %) for L3–L4]. However, while the sum of forces in MF, LTpL, and ILpL (local muscles) decreased at L3–L4 by 105 N (55 %), it increased at L1–L2 by 23 N (53 %).

Discussion

We used a dynamic musculoskeletal model of the lumbar spine to study the effect of muscle damage on spinal loading, specifically at the adjacent levels. Muscle damage was simulated by detaching the muscle fascicles, as they are often resected from the vertebrae during surgery. The two scenarios, one without and one with spinal fusion, both led to increased loading at both adjacent levels during neutral standing. This suggests the possible role of muscle damage in altered loading and accelerated degeneration of the disc adjacent to the lumbar spinal fusion, independent of the type of surgical fixation.

Our results demonstrated that with muscle damage, larger increases in axial forces occurred at the rostral adjacent level (78 % in presence of fixation and 73 % without fixation) in comparison to the caudal level (41 % in presence of fixation and 32 % without fixation). This is interesting as both radiographic and symptomatic adjacent segment degeneration are reported clinically to mostly occur at the rostral level [5, 61–64]. Given that animal studies have demonstrated increased degenerative changes at the disc under increased compressive loads [8–12], our results are consistent with these clinical observations.

To further investigate the reason for a larger increase in axial force at the rostral adjacent level, we provide the following simple geometric model for the entire spine that analytically predicts similar results. Consider the spine as a rigid bar that is hinged to the sacrum at the L5–S1 joint (Fig. 8). If a force *W* representing the body weight is applied at the tip of the bar, to keep the bar at equilibrium, a force representing the resultant of muscle forces should be applied in a way to cancel out the moment caused by the force *W* about the hinge joint.

To study the effect of lumbar muscle damage on spinal loads, we considered two cases: in Case 1, the force

Fig. 6 Predicted spinal loads at all lumbar intervertebral levels for No Fusion scenario. Forces are in N, moments are in Nm, and positive values for shear forces point to the anterior direction

Muscles Intact				Muscles Damaged			
	Axial Force	Shear Force	Flexion Moment		Axial Force	Shear Force	Flexion Moment
L1-L2	658	-285	2.0		1141	-496	-0.5
L2-L3	796	-272	0.2		1268	-326	-0.6
L3-L4	893	-228	-0.9		1324	-179	-0.4
L4-L5	984	-44	-1.4		1365	135	-0.4
L5-S1	959	331	-1.2		1266	613	-0.3

The Amount of Increase in Loads After Injury			
	Axial Force	Shear Force	Flexion Moment
L1-L2	483	-211	-2.5
L2-L3	472	-54	-0.8
L3-L4	431	49	0.5
L4-L5	381	179	1.0
L5-S1	307	282	0.9

representing the resultant of local muscles (attached to the lumbar spine) is applied at the middle of the bar (Fig. 8b), while in Case 2, the force representing the global muscles (attached to the thoracic spine) is applied at the tip of the bar (Fig. 8c). We also assume the direction of the forces is such that they meet at the same point (i.e., point P such that $\overline{OM} = \overline{PM} = \overline{MT}$ and $\theta_1 = 2\theta_2$) (see Fig. 8a). Solving this simple system (equations shown in Fig. 8) yields the ratio between F_2 and F_1 as a function of θ_2 only and does not depend on the angle the bar makes with horizontal line (Fig. 9). Note that F_2 and F_1 represent the muscle forces and are thus proportional to the axial forces in the spine. For small angles of θ_2 (i.e., $<20^\circ$) the ratio between the axial forces is less than 1.15 (blue line in Fig. 9). This means that for small muscle angles, whether F_1 (representing local muscles) or F_2 (representing global muscles) is maintaining the balance of the bar, the axial force at L5–S1 (point O in Fig. 8a) will not be very different. This links with the small increase (32 %) observed at the caudal adjacent segment when lumbar muscles were damaged in the computational model.

However, the situation becomes different at the rostral level with muscle damage. In case 2, the axial force due to global muscles ($F_2 \cos \theta_2$) is applied along the entire bar. In contrast, in case 1, the axial force due to local muscles ($F_1 \cos \theta_1$) starts from the middle of the bar and thus is applied only over the lower half. Therefore, if we assume L1–L2 being located above the middle point, in case 1 there is no axial force on L1–L2, whereas in case 2, there is axial force applied by F_2 . Thus, with damage to the local muscles, the overall spine loading becomes more like Case 2 and this explains the observed larger axial force at the rostral adjacent level (73 %) in the computational model.

To the best of our knowledge, the effect of muscle damage on spinal loading has not been investigated

previously. One study investigated the effect of muscle damage on muscle activations pattern, but did not report on spinal loading [48]. In that study, Bresnahan et al. [48] used the model developed by de Zee et al. [45] and simulated the muscle damage by successively reducing the CSA of the damaged muscles at L3–L5 by 10, 30, and 40 % from all posterior muscles (multifidus, LTP, ILpL, LTP, ILpT). They observed that accordingly, the activation of erector spinae muscle changed in flexion–extension and lateral bending, but the change was largest in axial rotation. However, they did not measure the spinal loads; and intervertebral disc stiffness, ligaments, and muscle force–length and force–velocity curves were not incorporated in their model.

Muscle force–length curves and nonlinear stiffness of the functional spinal units were implemented in our model. Also, the motions of the lumbar vertebrae were not predefined as a function/fraction of the total lumbar spine motion, which was done in the studies by de Zee et al. [45], Han et al. [47], and Christophy et al. [46]. This feature allowed each vertebra to move independently and was necessary for modeling the rigid fixation, which would alter the motion function. Finally, in contrast to Bresnahan [48], in our model muscle damage was simulated by detaching the injured fascicles rather than uniformly reducing the CSAs of all posterior muscles. Detaching muscles led to nonuniform reduction in CSAs of posterior muscles and varied between levels (see Fig. 7b). Despite these strengths, our model had some limitations that need future improvement.

As addressed in the study by Malakoutian et al. [49], one major limitation of the model was the sensitivity of the spinal forces to kinematic input. However, our study was focused on addressing the relative effect of muscle damage on forces and thus changes in the absolute force

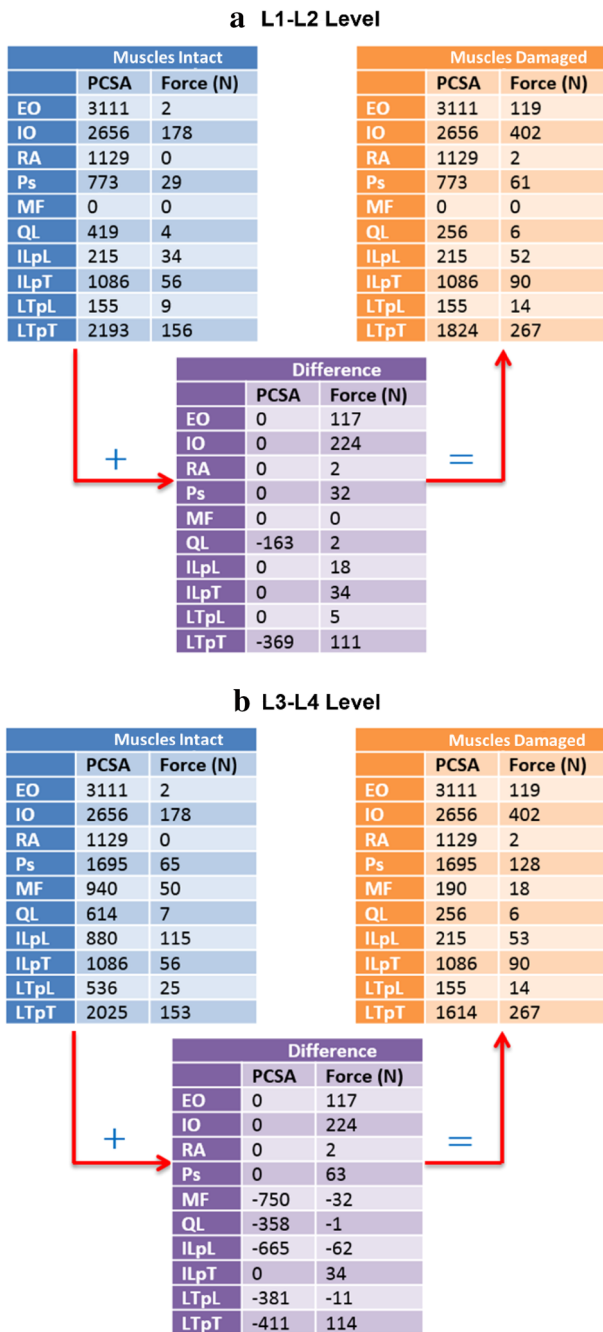


Fig. 7 **a** Physiological cross-sectional area (PCSA) and force of each muscle group crossing L1–L2 level for No Fusion scenario. PCSA is in mm². **b** Physiological cross-sectional area (PCSA) and force of each muscle group crossing L3–L4 level for No Fusion scenario. PCSA is in mm². EO external oblique, IO internal oblique, RA rectus abdominis, Ps psoas major, MF multifidus, QL quadratus lumborum, ILpL iliocostalis lumborum pars lumborum, ILpT iliocostalis lumborum pars thoracis, LTpL longissimus thoracis pars lumborum, LTpT longissimus thoracis pars thoracis

magnitudes were unlikely to alter the observed percentage changes. Other limitations of the model included assuming straight lines between the remaining attachment points of

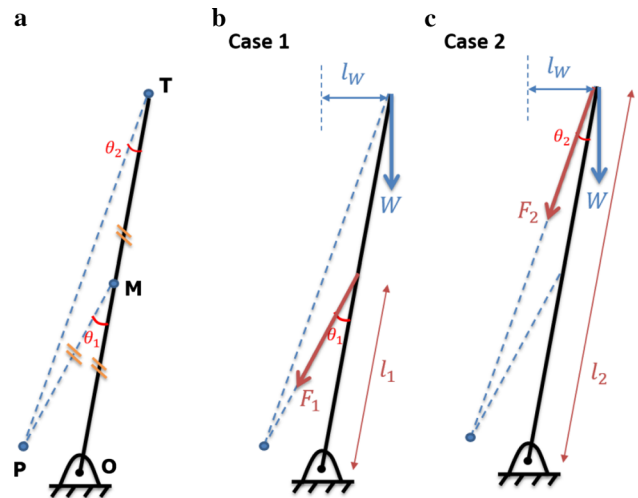


Fig. 8 A simple analytical model of the spine. **a** The spine is modeled as a rigid bar hinged at L5–S1 joint (point O). **b** Case 1 represents a spine maintained at equilibrium by the resultant of local muscles, while in case 2 **c**, the resultant of the global muscles is keeping the spine upright. The equilibrium equations mandate that $F_1 = \frac{Wl_w}{l_1 \sin \theta_1}$ and $F_2 = \frac{Wl_w}{l_2 \sin \theta_2}$

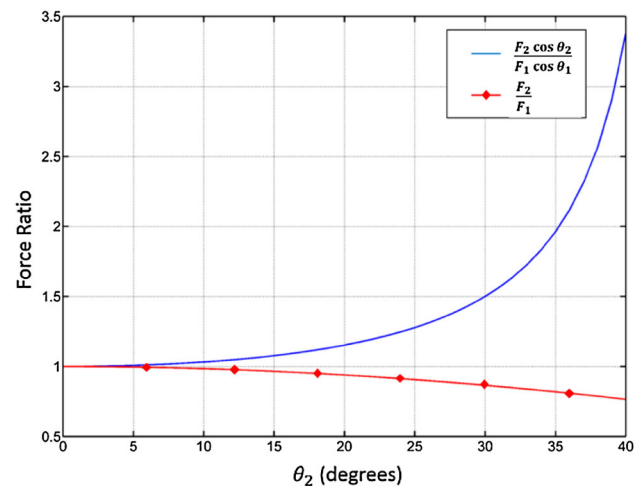


Fig. 9 The ratios of muscle forces and their axial components between case 1 and case 2 as a function of θ_2 . The ratios are obtained as: $\frac{F_2}{F_1} = \frac{l_1 \sin \theta_1}{l_2 \sin \theta_2} = \frac{l_1 (2 \sin \theta_2 \cos \theta_2)}{l_2 \sin \theta_2} = \cos \theta_2$ and $\frac{(F_2)_{axial}}{(F_1)_{axial}} = \frac{F_2 \cos \theta_2}{F_1 \cos \theta_1} = \frac{l_1 \tan \theta_1}{l_2 \tan \theta_2} = \frac{1}{2} \frac{\tan 2\theta_2}{\tan \theta_2} = \frac{1}{2} \frac{2 \tan \theta_2}{(1 - \tan^2 \theta_2) \tan \theta_2} = \frac{1}{1 - \tan^2 \theta_2}$

injured muscles (Fig. 3), neglecting off-diagonal terms of the stiffness matrix of the functional spinal units, and not considering the mechanical stability of the model into the system equations, which should be considered in the future versions of the model.

The current study only simulated severe muscle damage at three vertebral levels (L2–L5) and the fusion/fixation was assumed to be rigid. Also, only the case of upright standing was studied. Obviously, different degrees and lengths of muscle damage, in addition to other tasks and

postures, should be investigated in the future to tease out the effects of muscle dysfunction in specific spinal pathologies. We only modeled iatrogenic muscle damage and we did it by detaching the muscles from the treated levels. Other forms of muscle damage simulation can include adding the effect of fat infiltration and scar tissue or considering adaptive changes in architecture and mechanical properties of the muscle. Investigation of the effects of fixations with different stiffness is also of high interest to clinicians, although we do not expect a significant effect given the observation herein of the force changes without any fusion being present.

In conclusion, the findings of the present study suggest that the paraspinal muscles of the lumbar spine may play an important role in the etiology of adjacent segment changes beside a spinal fusion and that this effect is independent of spinal instrumentation. This observation is consistent with those studies that have observed decreased disc height at the adjacent level [7]. Further, the finding is consistent with those investigators who suggest that anterior approaches that spare the posterior musculature may have a role in reducing the development of adjacent level changes [2, 65].

Acknowledgments The authors gratefully acknowledge financial support from the Natural Sciences and Engineering Research Council of Canada (NSERC).

Compliance with ethical standards

Conflict of interest None.

References

- Park P, Garton HJ, Gala VC et al (2004) Adjacent segment disease after lumbar or lumbosacral fusion: review of the literature. *Spine (Phila Pa 1976)* 29:1938–1944
- Wai EK, Santos ERG, Morcom RA, Fraser RD (2006) Magnetic resonance imaging 20 years after anterior lumbar interbody fusion. *Spine (Phila Pa 1976)* 31:1952–1956
- Axelsson P, Johnsson R, Strömqvist B (2007) Adjacent segment hypermobility after lumbar spine fusion after surgery. *Acta Orthop* 78:834–839. doi:10.1080/17453670710014635
- Seitsalo S, Schlenzka D (1997) Disc degeneration in young patients with isthmic spondylolisthesis treated operatively or conservatively: a long-term follow-up. *Eur Spine J* 6:393–397
- Korovessis P, Repantis T, Zacharatos S, Zafropoulos A (2009) Does Wallis implant reduce adjacent segment degeneration above lumbosacral instrumented fusion? *Eur Spine J* 18:830–840. doi:10.1007/s00586-009-0976-y
- Kaito T, Hosono N, Mukai Y et al (2010) Induction of early degeneration of the adjacent segment after posterior lumbar interbody fusion by excessive distraction of lumbar disc space. *J Neurosurg Spine* 12:671–679. doi:10.3171/2009.12.SPINE08823
- Mannion AF, Leivseth G, Brox J-I, et al. (2014) Long-term follow up suggests spinal fusion is associated with increased adjacent segment disc degeneration but without influence on clinical outcome: results of a combined follow-up from 4 RCTs. *Spine (Phila Pa. 1976)* 39:1373–83. doi:10.1097/BRS.0000000000000437
- Lotz JC, Chin JR (2000) Intervertebral disc cell death is dependent on the magnitude and duration of spinal loading. *Spine (Phila Pa 1976)* 25:1477–1483
- Stokes IAF, Iatridis JC (2004) Mechanical conditions that accelerate intervertebral disc degeneration: overload versus immobilization. *Spine (Phila Pa 1976)* 29:2724–2732
- Walter BA, Korecki CL, Purmessur D et al (2011) Complex loading affects intervertebral disc mechanics and biology. *Osteoarthr Cartil* 19:1011–1018
- Chan SCW, Ferguson SJ, Gantenbein-Ritter B (2011) The effects of dynamic loading on the intervertebral disc. *Eur Spine J* 20:1796–1812
- Kim J, Yang S-J, Kim H et al (2012) Effect of shear force on intervertebral disc (IVD) degeneration: an in vivo rat study. *Ann Biomed Eng* 40:1996–2004
- Hodges PW, Richardson CA (1996) Inefficient muscular stabilization of the lumbar spine associated with low back pain: a motor control evaluation of transversus abdominis. *Spine (Phila Pa 1976)* 21:2640–2650
- Cholewicki J, Silfies SP, Shah RA et al (2005) Delayed trunk muscle reflex responses increase the risk of low back injuries. *Spine (Phila Pa 1976)* 30:2614–2620
- Lee AS, Cholewicki J, Reeves NP et al (2010) Comparison of trunk proprioception between patients with low back pain and healthy controls. *Arch Phys Med Rehabil* 91:1327–1331
- Tsao H, Tucker KJ, Hodges PW (2011) Changes in excitability of corticomotor inputs to the trunk muscles during experimentally-induced acute low back pain. *Neuroscience* 181:127–133
- Haig AJ, London Z, Sandella DE (2013) Symmetry of paraspinal muscle denervation in clinical lumbar spinal stenosis: support for a hypothesis of posterior primary ramus stretching? *Muscle Nerve* 48:198–203
- Leinonen V, Määttä S, Taimela S et al (2003) Paraspinal muscle denervation, paradoxically good lumbar endurance, and an abnormal flexion–extension cycle in lumbar spinal stenosis. *Spine (Phila Pa 1976)* 28:324–331
- Wang G, Karki SB, Xu S et al (2014) Quantitative MRI and X-ray analysis of disc degeneration and paraspinal muscle changes in degenerative spondylolisthesis. *J Back Musculoskelet Rehabil.* doi:10.3233/BMR-140515
- Gejo R, Matsui H, Kawaguchi Y et al (1999) Serial changes in trunk muscle performance after posterior lumbar surgery. *Spine (Phila Pa 1976)* 24:1023–1028
- Kawaguchi Y, Matsui H, Gejo R, Tsuji H (1998) Preventive measures of back muscle injury after posterior lumbar spine surgery in rats. *Spine (Phila Pa 1976)* 23:2282–2287
- Kawaguchi Y, Matsui H, Tsuji H (1996) Back muscle injury after posterior lumbar spine surgery: a histologic and enzymatic analysis. *Spine (Phila Pa 1976)* 21:941–944
- Cawley DT, Alexander M, Morris S (2014) Multifidus innervation and muscle assessment post-spinal surgery. *Eur Spine J* 23:320–327
- Keller A, Gunderson R, Reikerås O, Brox JI (2003) Reliability of computed tomography measurements of paraspinal muscle cross-sectional area and density in patients with chronic low back pain. *Spine (Phila Pa 1976)* 28:1455–1460. doi:10.1097/01.BRS.0000067094.55003.AD
- Keller A, Brox JI, Gunderson R et al (2003) Trunk muscle strength, cross-sectional area, and density in patients with chronic low back pain randomized to lumbar fusion or cognitive intervention and exercises. *Spine (Phila Pa 1976)* 29:3–8
- Wang H-L, Lu F-Z, Jiang J-Y et al (2011) Minimally invasive lumbar interbody fusion via MAST Quadrant retractor versus open surgery: a prospective randomized clinical trial. *Chin Med J-Beijing* 124:3868
- Kramer M, Katzmaier P, Eisele R et al (2001) Surface electromyography-verified muscular damage associated with the

- open dorsal approach to the lumbar spine. *Eur Spine J* 10:414–420
28. Kim D-Y, Lee S-H, Chung SK, Lee H-Y (2004) Comparison of multifidus muscle atrophy and trunk extension muscle strength: percutaneous versus open pedicle screw fixation. *Spine (Phila Pa 1976)* 30:123–129
 29. Mayer TG, Vanharanta H, Gatchel RJ et al (1989) Comparison of CT scan muscle measurements and isokinetic trunk strength in postoperative patients. *Spine (Phila Pa 1976)* 14:33–36
 30. Panjabi MM (2007) Hybrid multidirectional test method to evaluate spinal adjacent-level effects. *Clin Biomech (Bristol, Avon)* 22:257–265. doi:[10.1016/j.clinbiomech.2006.08.006](https://doi.org/10.1016/j.clinbiomech.2006.08.006)
 31. Malakoutian M, Volkheimer D, Street J et al (2015) Do in vivo kinematic studies provide insight into adjacent segment degeneration?—a qualitative systematic literature review. *Eur Spine J* 24:1865–1881
 32. Anderst WJ, Donaldson WF, Lee JY, Kang JD (2013) Cervical spine intervertebral kinematics with respect to the head are different during flexion and extension motions. *J Biomech* 46:1471–1475
 33. Volkheimer D, Malakoutian M, Oxland TR, Wilke H-J (2015) Limitations of current in vitro test protocols for investigation of instrumented adjacent segment biomechanics: critical analysis of the literature. *Eur J Spine* 24:1882–1892
 34. Weinhoffer SL, Guyer RD, Herbert M, Griffith SL (1995) Intradiscal pressure measurements above an instrumented fusion: a cadaveric study. *Spine (Phila Pa 1976)* 20:526–531
 35. Chow DHK, Luk KDK, Evans JH, Leong JCY (1996) Effects of short anterior lumbar interbody fusion on biomechanics of neighboring unfused segments. *Spine (Phila Pa 1976)* 21:549–555
 36. Cunningham BW, Kotani Y, McNulty PS et al (1997) The effect of spinal destabilization and instrumentation on lumbar intradiscal pressure: an in vitro biomechanical analysis. *Spine (Phila Pa 1976)* 22:2655–2663
 37. Pfeiffer M, Hoffman H, Goel VK et al (1997) In vitro testing of a new transpedicular stabilization technique. *Eur Spine J* 6:249–255
 38. Bastian L, Lange U, Knop C et al (2001) Evaluation of the mobility of adjacent segments after posterior thoracolumbar fixation: a biomechanical study. *Eur Spine J* 10:295–300
 39. Schmoelz W, Huber JF, Nydegger T et al (2003) Dynamic stabilization of the lumbar spine and its effects on adjacent segments: an in vitro experiment. *J Spinal Disord Tech* 16:418–423
 40. Moore J, Yoganandan N, Pintar FA et al (2006) Tapered cages in anterior lumbar interbody fusion: biomechanics of segmental reactions. *J Neurosurg Spine* 5:330–335
 41. Schmoelz W, Huber JF, Nydegger T et al (2006) Influence of a dynamic stabilisation system on load bearing of a bridged disc: an in vitro study of intradiscal pressure. *Eur Spine J* 15:1276–1285
 42. McGill SM, Norman RW (1986) Partitioning of the L4–L5 dynamic moment into disc, ligamentous, and muscular components during lifting. *Spine (Phila Pa 1976)* 11:666–678
 43. Stokes IAF, Gardner-Morse M (1995) Lumbar spine maximum efforts and muscle recruitment patterns predicted by a model with multijoint muscles and joints with stiffness. *J Biomech* 28:173–186
 44. Arjmand N, Shirazi-Adl A (2006) Model and in vivo studies on human trunk load partitioning and stability in isometric forward flexions. *J Biomech* 39:510–521. doi:[10.1016/j.jbiomech.2004.11.030](https://doi.org/10.1016/j.jbiomech.2004.11.030)
 45. de Zee M, Hansen L, Wong C et al (2007) A generic detailed rigid-body lumbar spine model. *J Biomech* 40:1219–1227. doi:[10.1016/j.jbiomech.2006.05.030](https://doi.org/10.1016/j.jbiomech.2006.05.030)
 46. Christophy M, Faruk Senan NA, Lotz JC, O'Reilly OM (2012) A musculoskeletal model for the lumbar spine. *Biomech Model Mechanobiol* 11:19–34. doi:[10.1007/s10237-011-0290-6](https://doi.org/10.1007/s10237-011-0290-6)
 47. Han K-S, Zander T, Taylor WR, Rohlmann A (2012) An enhanced and validated generic thoraco-lumbar spine model for prediction of muscle forces. *Med Eng Phys* 34:709–716. doi:[10.1016/j.medengphy.2011.09.014](https://doi.org/10.1016/j.medengphy.2011.09.014)
 48. Bresnahan L, Fessler RG, Natarajan RN (2010) Evaluation of change in muscle activity as a result of posterior lumbar spine surgery using a dynamic modeling system. *Spine (Phila Pa 1976)* 35:E761–E767. doi:[10.1097/BRS.0b013e3181e45a6e](https://doi.org/10.1097/BRS.0b013e3181e45a6e)
 49. Malakoutian M, Street J, Wilke H-J et al (2015) A musculoskeletal model of the lumbar spine using ArtiSynth—development and validation. *Comput Methods Biomech Biomed Eng Imag Vis* 1–8. doi:[10.1080/21681163.2016.1187087](https://doi.org/10.1080/21681163.2016.1187087)
 50. Lloyd JE, Stavness I, Fels S (2012) ArtiSynth: A fast interactive biomechanical modeling toolkit combining multibody and finite element simulation. In: *Soft Tissue Biomechanical Modeling for Computer Assisted Surgery*. Springer, pp 355–394. doi:[10.1007/8415_2012_126](https://doi.org/10.1007/8415_2012_126)
 51. Stavness I, Lloyd JE, Payan Y, Fels S (2011) Coupled hard–soft tissue simulation with contact and constraints applied to jaw–tongue–hyoid dynamics. *Int J Numer Method Biomed Eng* 27:367–390
 52. Stavness I, Lloyd JE, Fels S (2012) Automatic prediction of tongue muscle activations using a finite element model. *J Biomech* 45:2841–2848
 53. Dao TT, Pouletaut P, Charleux F, Lazáry Á, Eltes P, Varga PP, Tho MC (2014) Estimation of patient specific lumbar spine muscle forces using multi-physical musculoskeletal model and dynamic MRI. In: Huynh VN, Denoex T, Tran DH, Le AC, Pham SB (eds) *Knowledge and Systems Engineering vol. 2, Advances in Intelligent Systems and Computing*. Springer International Publishing, Cham, pp 411–422. doi:[10.1007/978-3-319-02821-7_36](https://doi.org/10.1007/978-3-319-02821-7_36)
 54. Panjabi MM, Brand RA Jr, White AA III (1976) Three-dimensional flexibility and stiffness properties of the human thoracic spine. *J Biomech* 9:185–192
 55. Heuer F, Schmidt H, Klezl Z et al (2007) Stepwise reduction of functional spinal structures increase range of motion and change lordosis angle. *J Biomech* 40:271–280
 56. Gardner-Morse MG, Stokes IA (2004) Structural behavior of human lumbar spinal motion segments. *J Biomech* 37:205–212. doi:[10.1016/j.jbiomech.2003.10.003](https://doi.org/10.1016/j.jbiomech.2003.10.003)
 57. Millard M, Uchida T, Seth A, Delp SL (2013) Flexing computational muscle: modeling and simulation of musculotendon dynamics. *J Biomech Eng* 135:21005
 58. Cobb WS, Burns JM, Kercher KW et al (2005) Normal intradiscal pressure in healthy adults. *J Surg Res* 129:231–235
 59. Stavness IK (2010) *Byte your tongue*. PhD dissertation, University of British Columbia
 60. Wilke H-J, Neef P, Hinz B et al (2001) Intradiscal pressure together with anthropometric data—a data set for the validation of models. *Clin Biomech* 16:S111–S126
 61. Poh S-Y, Yue W-M, Chen JL-T et al (2011) Two-year outcomes of transforaminal lumbar interbody fusion. *J Orthop Surg* 19:135–140
 62. Min J-H, Jang J-S, Lee S-H (2007) Comparison of anterior-and posterior-approach instrumented lumbar interbody fusion for spondylolisthesis. *J Neurosurg Spine* 7(1):21–26
 63. Chou W-Y, Hsu C-J, Chang W-N, Wong C-Y (2002) Adjacent segment degeneration after lumbar spinal posterolateral fusion with instrumentation in elderly patients. *Arch Orthop Trauma Surg* 122:39–43
 64. Yee TJ, Terman SW, La Marca F, Park P (2014) Comparison of adjacent segment disease after minimally invasive or open transforaminal lumbar interbody fusion. *J Clin Neurosci Off J Neurosurg Soc Australas* 21(10):1796–1801
 65. Kim H-J, Moon S-H, Chun H-J et al (2009) Comparison of mechanical motion profiles following instrumented fusion and non-instrumented fusion at the L4–5 segment. *Clin Invest Med* 32:E64–E69